Computer Physics Communications 182 (2011) 68–70

Contents lists available at ScienceDirect

Computer Physics Communications

www.elsevier.com/locate/cpc

Low-energy electronic structures of nanotube–nanoribbon hybrid systems

C.H. Lee [a], S.C. Chen [b], C.K. Yang [a], W.S. Su [b,*], M.F. Lin [b,*]

[a] Center for General Education, Chang Gung University, Kueishan, Taiwan, ROC
[b] Department of Physics, National Cheng Kung University, Tainan, Taiwan, ROC

ARTICLE INFO

Article history:
Received 28 February 2010
Received in revised form 15 June 2010
Accepted 14 July 2010
Available online 21 July 2010

Keywords:
Carbon nanotube
Graphene nanoribbon
Electronic properties

ABSTRACT

The electronic properties of a nanotube–nanoribbon hybrid system are investigated by the first-principles calculations. This hybrid system is constructed by a zigzag carbon nanotube and an armchair graphene nanoribbon. Its electronic structures strongly depend on the nanotube location and stacking configuration. The interactions between the two subsystems would break the state degeneracy, open subband spacings, and induce more band-edge states. The predicted results could be measured directly by the scanning tunneling spectroscopy.

1. Introduction

The graphite-related systems have attracted much attention over the past decades. For example, a single-walled carbon nanotube (SWCNT) is a rolled-up graphite sheet in a seamless cylindrical form, first synthesized and observed in 1991 by Iijima [1]. The structure is specified by a circumferential vector $\mathbf{R}_x = m\mathbf{a}_1 + n\mathbf{a}_2$, where $\mathbf{a}_1$ and $\mathbf{a}_2$ are primitive lattice vectors of a graphite sheet [2]. The radius and chiral angle of a (m, n) carbon nanotube are, respectively, $r = b\sqrt{3(m^2 + mn + n^2)}/2\pi$ and $\theta = \tan^{-1}[-\sqrt{3}/(2m + n)]$ (b is the C–C distance). The electronic properties of the SWCNTs reveal the quasi-one-dimensional (Q1D) characteristics and are expected to be related with those of the monolayer graphene. They are either metal or semiconductor depending on the radius and chirality [2–4]. There are three types of carbon nanotubes according to their gaps. A (m, n) CNT is the gapless metal for $m = n$. For $2m + n \neq 3I$ (I an integer), the CNTs own moderate gaps whose magnitudes are $1/r$ dependence. The CNTs with $2m + n = 3I$ and $m \neq n$ would open narrow gaps due to the curvature effects, the misorientation of $2p_z$ orbitals and the hybridization of π and σ electrons. These gaps are inversely proportional to r^2.

The graphene nanoribbons (GNRs), associated with monolayer graphene, are also another Q1D system. They can be regarded as the elongated strips of graphene layer with finite width in a certain direction, and produced by the physical treatment and chemical synthesis [5–10]. The width and edge structure of GNRs dominate their electronic properties. The ribbon width is defined as the number of dimer or zigzag lines (N_y) along the transverse direction. The armchair and zigzag GNRs, with the former possessing armchair structure and the latter zigzag structure along the longitudinal direction, have been widely studied. Predicted by the tight-binding model [11,12] and the density-functional theory (DFT) [13–16], the armchair GNRs display the gap oscillations as a function of widths. However, the apparent difference between them is that the $N_y = 3I + 2$ armchair GNRs are metallic by the tight-binding model but will open gaps in the DFT calculations. On the other hand, the zigzag GNRs own the partial flat bands, which are contributed by the edge carbon atoms [12,17]. Further considering the spin orientation at the edge atoms, there exist two metastable configurations in the zigzag GNRs [18,19]. The ferromagnetic (FM) configuration means that the spins of the atoms on both sides parallel each other, whereas the antiferromagnetic (AFM) configuration denotes that the spins are antiparallel. Besides, the partial flat bands intersect or separate at the Fermi Level (E_F) corresponding to the FM or AFM configurations, respectively.

The multi-layered sp^2 systems, such as few-layer graphenes, multi-walled carbon nanotubes, and carbon nanotube bundles, are affected by the interactions of adjacent layers [20–24]. The interlayer atomic interactions also play an important role in the hybrid systems. For example, the systems consisting of CNT and GNR have been investigated by the tight-binding model [25,26]. These studies indicate that the interactions between the two subsystems modify the band structures, such as the destruction of state degeneracy and the occurrence of new band-edge states. The energy-gap modulation by means of the interlayer atomic interactions in the hybrid system is worthy to be examined.

* Corresponding authors.
E-mail addresses: xyzsheng@yahoo.com.tw (W.S. Su), mflin@mail.ncku.edu.tw (M.F. Lin).

0010-4655/$ – see front matter
doi:10.1016/j.cpc.2010.07.028

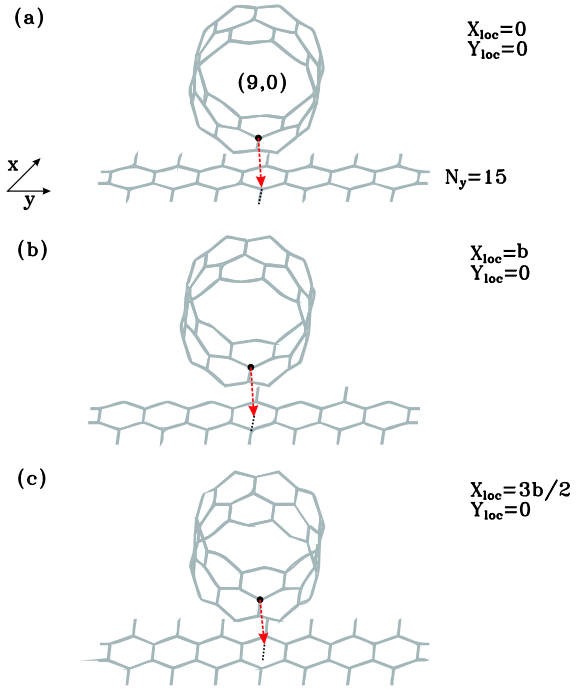

Fig. 1. The $(9,0)$ zigzag carbon nanotube on the $N_y = 15$ armchair graphene nanoribbon. The former is situated at (a) ($X_{loc} = 0$, $Y_{loc} = 0$), (b) $(b,0)$, and (c) $(3b/2,0)$.

2. Theory

Our calculations are performed by the density-functional theory with the Vienna *ab initio* simulation package (VASP). The exchange–correlation of electrons is treated within the generalized gradient approximation, as implemented by Perdew–Burke–Ernzerhof [27]. The cutoff energy for the expansion of wave functions and potentials in the plane-wave basis is chosen to be 500 eV. The Brillouin zone sampling is adopted with a grid of $1 \times 1 \times 80$. The atomic relaxation is carried out until the Helmann–Feynman forces are less than 0.01 eV/Å. The vacuum layer in the supercell used in our calculations is set to be 10 Å, large enough to minimize the artificial interlayer interactions.

In this hybrid system, the $(9,0)$ zigzag carbon nanotube lies on the armchair graphene nanoribbon. The width of the GNR is $N_y = 15$, defined as the number of dimer lines along the y-axis. b is the C–C bond length and $a = \sqrt{3}b$ is the length of the primitive unit vectors in the graphite sheet. There are 66 carbon atoms and 4 hydrogen atoms in this unit cell. As shown in Fig. 1(a), the C–C bonds from the bottom of CNT are projected directly onto the C–C bonds at the center of the ribbon. This arrangement is regarded as AA stacking and the nanotube location on the ribbon is assumed as $X_{loc} = 0$ and $Y_{loc} = 0$. After moving CNT along the x-axis with b, another configuration AB stacking arises, as presented in Fig. 1(b). One atom of the C–C bond is projected onto the carbon atom of the ribbon, and another is projected onto the center of the hexagonal lattice, usually found in bulk graphite. Another notable configuration is called the AA′ stacking at $X_{loc} = 3b/2$ and $Y_{loc} = 0$ [Fig. 1(c)]. It is similar to AA′ graphite, where alternate planes are shifted by half the hexagon width [28]. The interlayer spacing between the carbon nanotube and graphene nanoribbon is presumed as 3.15 Å. Complete relaxation of the combined structure of the CNT and the GNR is attained. After relaxation, the spacing between them in AB stacking remains unchanged, whereas that of AA stacking increases to 3.26 Å.

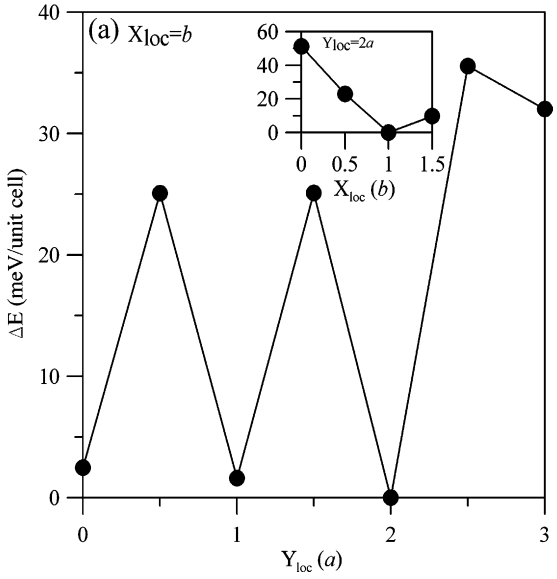

Fig. 2. The total energy difference per unit cell as a function of the nanotube location Y_{loc} with (a) $X_{loc} = b$. The total energies are relative to those of the configuration with the location ($X_{loc} = b$, $Y_{loc} = 2a$). The inset is the energy difference as a function of the location X_{loc} at $Y_{loc} = 2a$.

3. Results

The dependence of the total energy on the nanotube location is discussed. The total energy differences are relative to the location ($X_{loc} = b$, $Y_{loc} = 2a$), which is the most favorable in our calculations [Fig. 2(a)]. At $X_{loc} = b$, the total energy exhibits an oscillatory behavior as Y_{loc} increases. When the CNT lies on the center of the ribbon, as illustrated in Fig. 1(b) with the AB stacking, there exists the lower total energy and reveals more stable. The total energy increases about 22 meV per unit cell after the CNT is moved with $a/2$ toward y-axis. At $Y_{loc} = a$, the total energy reduces because the AB stacking is formed again. As the CNT gradually becomes closer to the edge of the ribbon, the total energy declines. However, when Y_{loc} is above $2a$, the total energy is drastically raised even in AB stacking.

The effects of the stacking configuration are investigated further, as shown in the inset of Fig. 2(a). The Y_{loc} is set at $2a$ and we change X_{loc} from 0 to $3b/2$. The AA stacking ($X_{loc} = 0$, $Y_{loc} = 2a$), as presented in Fig. 1(a), owns the highest total energy among these stacking configurations. This shows that the hybrid system with the AA stacking is unstable. On the contrary, there exists a metastable configuration at ($X_{loc} = 3b/2$, $Y_{loc} = 2a$), which denotes the AA′ stacking, as illustrated in Fig. 1(c).

We first discuss the low-energy band structures of two systems in the absence of the interlayer atomic interactions. As to the armchair GNR of $N_y = 15$, the 1D subbands have also parabolic dispersions. Besides, a moderate energy gap occurs at $k_x = 0$. However, an isolated $(9,0)$ zigzag CNT possesses a narrow energy gap opening near the $E_F = 0$, owing to the curvature effects [the inset of Fig. 3(a)]. Meanwhile, these energy bands nearest to E_F originating from the $(9,0)$ CNT are double degeneracy. With interlayer atomic interactions, the band structures are dramatically altered, such as the change of subband curvature and energy gap [Fig. 3(b)]. The state degeneracy is also broken by the interactions between the two subsystems. After changing Y_{loc} to $2a$, the band structures are slightly modified, as illustrated in Fig. 3(c). The nanotube location mainly affects the energy bands derived from the GNR. On the other hand, the stacking configuration also influences the low-energy electronic properties [Figs. 3(d)–3(f)]. It could be found that the degenerate bands close to the E_F are split evidently in the AA and AA′ stacking.

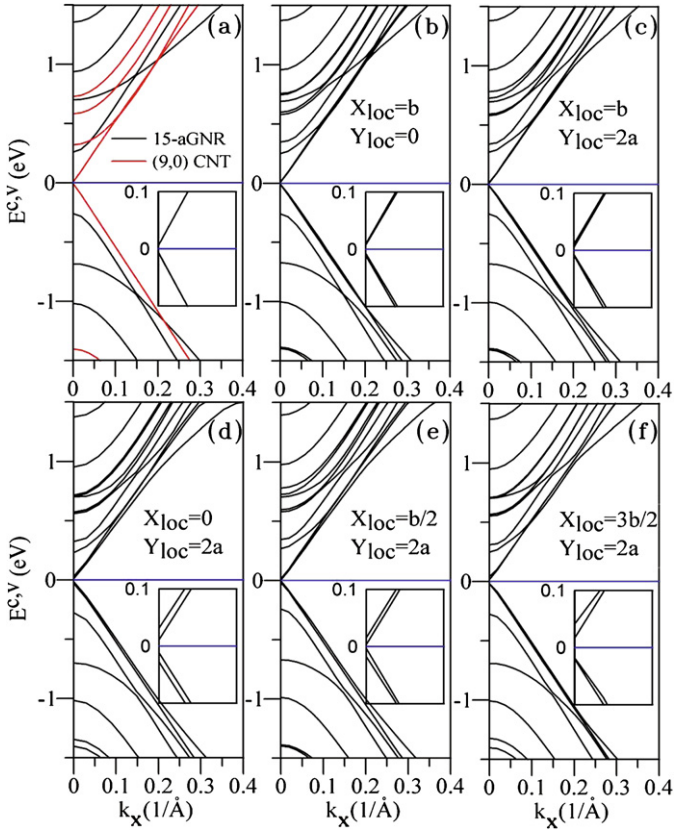

Fig. 3. The band structures of the nanotube location (X_{loc}, Y_{loc}) (b) $(b, 0)$, (c) $(b, 2a)$, (d) $(0, 2a)$, (e) $(b/2, 2a)$, and (f) $(3b/2, 2a)$. The bands of the isolated $(9, 0)$ CNT and $N_y = 15$ armchair GNR are also shown in (a).

4. Conclusion

The density-functional theory is performed to calculate the structural and electronic properties of nanotube–nanoribbon hybrid. The hybrid consists of zigzag $(9, 0)$ carbon nanotube on an armchair graphene nanoribbon with $N_y = 15$. The most stable arrangement occurs when the tube approaches the border of the ribbon and forms the AB-stacked configuration. The interlayer interactions would destroy the state degeneracy from the $(9, 0)$ carbon nanotube, induce more band-edge states, and vary the energy gap. Moreover, the different stacking configuration also play an important role. The optical absorption spectrum and transport measurements would provide powerful tools to observe the above-mentioned effects.

Acknowledgements

This work was supported by the NSC and NCTS of Taiwan, under the grant No. NSC 98-2112-M-006-013-MY4. We are grateful to the National Center for High-performance Computing for computer time and facilities.

References

[1] S. Iijima, Nature (London) 354 (1991) 56.
[2] R. Saito, M. Fujita, G. Dresselhaus, M.S. Dresselhaus, Appl. Phys. Lett. 60 (1992) 2204;
R. Saito, M. Fujita, G. Dresselhaus, M.S. Dresselhaus, Phys. Rev. B 46 (1992) 1804.
[3] C.L. Kane, E.J. Mele, Phys. Rev. Lett. 78 (1997) 1932.
[4] F.L. Shyu, C.P. Chang, R.B. Chen, C.W. Chiu, M.F. Lin, Phys. Rev. B 67 (2003) 045405.
[5] M. Murakami, S. Iijima, S. Yoshimura, J. Appl. Phys. 60 (1986) 3856.
[6] M. Yudasaka, Y. Tasaka, M. Tanaka, H. Kamo, Y. Ohki, S. Usami, Appl. Phys. Lett. 64 (1994) 3237.
[7] B.L.V. Prasad, H. Sato, T. Enoki, Y. Hishiyama, Y. Kaburagi, A.M. Rao, P.C. Eklund, Kyoichi Oshida, Morinobu Endo, Phys. Rev. B 62 (2000) 11209.
[8] L. Tapasztó, G. Dobrik, Ph. Lambin, L.P. Biró, Nature Nanotech. 3 (2008) 397.
[9] D.V. Kosynkin, A.L. Higginbotham, A. Sinitskii, J.R. Lomeda, A. Dimiev, B.K. Price, J.M. Tour, Nature (London) 458 (2009) 872.
[10] L. Jiao, L. Zhang, X. Wang, G. Diankov, H. Dai, Nature (London) 458 (2005) 877.
[11] K. Nakada, M. Fujita, G. Dresselhaus, M.S. Dresselhaus, Phys. Rev. B 54 (1996) 17954.
[12] M. Ezawa, Phys. Rev. B 73 (2006) 045432.
[13] Y.-W. Son, M.L. Cohen, S.G. Louie, Phys. Rev. Lett. 97 (2003) 216803.
[14] V. Barone, O. Hod, G.E. Scuseria, Nano Lett. 6 (2006) 2749.
[15] L. Yang, C.-H. Park, Y.-W. Son, M.L. Cohen, S.G. Louie, Phys. Rev. Lett. 99 (2007) 186801.
[16] S. Okada, Phys. Rev. B 77 (2008) 041408(R).
[17] M. Fujita, K. Wakabayashi, K. Nakada, K. Kusakabe, J. Phys. Soc. Jpn. 65 (1996) 1920.
[18] Y.-W. Son, M.L. Cohen, S.G. Louie, Nature (London) 444 (2006) 347.
[19] L. Pisani, J.A. Chan, B. Montanari, N.M. Harrison, Phys. Rev. B 75 (2007) 064418.
[20] T. Ohta, A. Bostwick, T. Seyller, K. Horn, E. Rotenberg, Science 313 (2006) 951.
[21] S. Latil, L. Henrard, Phys. Rev. Lett. 97 (2006) 036803.
[22] M.F. Craciun, S. Russo, M. Yamamoto, J.B. Oostinga, A.F. Morpurgo, S. Tarucha, Nature Nanotech. 4 (2009) 383.
[23] Y.H. Ho, C.P. Chang, F.L. Shyu, R.B. Chen, S.C. Chen, M.F. Lin, Carbon 42 (2004) 3159.
[24] A. Thess, R. Lee, P. Nikolaev, H. Dai, P. Petit, J. Robert, C. Xu, Y.H. Lee, S.G. Kim, A.G. Rinzler, D.T. Colbert, G.E. Scuseria, D. Tománek, J.E. Fischer, R.E. Smalley, Science 273 (1996) 483.
[25] T.S. Li, S.C. Chang, J.Y. Lien, M.F. Lin, Nanotechnology 19 (2008) 105703.
[26] T.S. Li, S.C. Chang, M.F. Lin, Eur. Phys. J. B 70 (2009) 497.
[27] J.P. Perdew, K. Burke, M. Ernzerhof, Phys. Rev. Lett. 77 (2007) 3865.
[28] J.-K. Lee, S.-C. Lee, J.-P. Ahn, S.-C. Kim, J.I.B. Wilson, P. John, J. Chem. Phys. 129 (2008) 234709.